AIChE

# Continuous Process for Production of Hydrogenated Nitrile Butadiene Rubber Using a Kenics® KMX Static Mixer Reactor

**Chandra Mouli R. Madhuranthakam, Qinmin Pan, and Garry L. Rempel**
Dept. of Chemical Engineering, University of Waterloo, Waterloo, ON N2L 3G1, Canada

*DOI 10.1002/aic.11869*

*A continuous process for hydrogenating nitrile butadiene rubber (NBR) was developed and its performance was experimentally investigated. A Kenics® KMX static mixer (SM) is used in the process as a gas–liquid reactor in which gaseous hydrogen reacts with NBR in an organic solution catalyzed by an organometallic complex such as an osmium complex catalyst. The Kenics® KMX SM was designed with 24 mixing elements with 3.81 cm diameter and arranged such that the angle between two neighboring elements is 90°. The internal structure of each element is open blade with the blades being convexly curved. The dimensions of the SM reactor are: 3.81 cm ID 80 S and 123 cm length and was operated cocurrently with vertical upflow. The NBR solutions of different concentrations (0.418 and 0.837 mol/L with respect to [C=C]) were hydrogenated by using different concentrations of the osmium catalyst solution at various residence times. The reactions were conducted at a constant temperature of 138°C and at a constant pressure of 3.5 MPa. From the experimental results, it is observed that a conversion and/or degree of hydrogenation above 95% was achieved in a single pass from the designed continuous process. This is the first continuous process for HNBR production that gives conversions above 95% till date. Optimum catalyst concentration for a given mean residence time to achieve conversions above 95% were obtained. Finally, a mechanistic model for the SM reactor performance with respect to hydrogenation of NBR was proposed and validated with the obtained experimental results.* © 2009 American Institute of Chemical Engineers *AIChE J*, 55: 2934–2944, 2009

*Keywords: process synthesis, reactor analysis, HNBR, Kenics®, KMX static mixer, mathematical modeling*

## Introduction

Catalytic hydrogenation of nitrile butadiene rubber (NBR) is a postpolymerization process that alters and optimizes the chemical and physical properties of the parent polymer (NBR). Hydrogenated nitrile butadiene rubber (HNBR) is widely known for its physical strength and retention properties after long-time exposure to heat, oil and chemicals. The unique properties attributed to HNBR have resulted in wide adoption of HNBR as a high-performance elastomer in automotive, industrial and assorted, performance demanding applications. On a volume basis, the automotive industry is the largest consumer of HNBR using it for dynamic and static seals, hoses, and belts. Also, significant use is in oil exploration and processing, as well as rolls for steel and paper mills. Hydrogenation of NBR is currently carried out in the industry preferably via homogeneous catalysis. As yet, it is being produced in a semibatch process accompanied with hydrogen transfer from the gas to liquid phase. Several catalysts have been exploited successfully for the hydrogenation

---

Correspondence concerning this article should be addressed to G. L. Rempel at grempel@cape.uwaterloo.ca.

in organic solvents that include palladium, rhodium, ruthenium, iridium, and osmium complexes.[1] Ru- and Os-based catalytic processes are receiving more prominence due to their effectiveness and much cheaper catalyst cost than the Rh-based systems. Because of the huge demand for HNBR, the need for continuous production becomes important compared with the conventional batch production. Although batch processing is capable of achieving high-olefin conversions, it is disadvantageous in terms of throughput. When the throughput has to be increased, a batch process can no longer be favorable in terms of auxiliary costs such as processing the raw material for the reactor, time required to fill and empty the reactor which takes a significant fraction of production time. In addition to that, the heat produced in the continuous process can be integrated elsewhere in the process which is not possible with a batch process. Parent[2] and Kehl[3] showed that the continuous process is feasible through a plug flow reactor packed with nonporous ceramic saddles. The length to diameter ratio of the packed bed reactor was very high and is not favorable for scale up. Another drawback with the packed bed reactor was that a significant volume of the reactor is occupied by the packing material, which decreases the production yield. Pan et al.[4] have numerically shown that a reactor that can behave like a plug flow reactor with an instant mixing component (CSTR) at the inlet would be efficient for the earlier said purpose. As a continuation to their work (Madhuranthakam et al.[5]) have numerically showed that a static mixer (SM) reactor with open blade internal structure under certain optimal conditions would give very high conversions in the NBR system. SMs are tubular devices with mixing elements arranged such that each element is at 90° with its neighboring element. There are many different mixer geometries for various purposes and the performances of these have been studied experimentally and theoretically.[6–8] They are used for a wide variety of applications in the chemical process industries such as, in chlorination and oxidation, acid and base dilution, fast reactions, plug flow finishing reactors, thermal homogenization, reactant/catalyst blending, gasoline blending, water and waste treatment, pharmaceuticals.[9] When used as reactors they can assure plug flow behavior, good mass transfer, and heat transfer. Other advantages include low-maintenance cost, low-space requirements, and easy installation. For a system like a NBR solution, where the viscosity increases with the concentration of polymer, an internal structure with open blade design is favorable. Two important commercial open blade designs available and used for many applications in the chemical process industry are Sulzer® SMX and Kenics® KMX. The Sulzer® SMX element has intricate open blade design with flat blades and the Kenics® KMX design has identical structure except that the blades are concavely curved. With respect to mixing, Heniche et al.[10] showed that the Kenics® KMX structure is better than the Sulzer® SMX at the expense of a higher pressure drop. These SMs were commonly used only for mixing and/or blending polymers in the laminar flow regime and were mostly attributed to liquid–liquid phase applications. For the first time, a Kenics® KMX SM has been proposed and used as gas–liquid reactor for the postpolymerization of NBR to produce HNBR. There is no reported literature or technology that produces high-quality HNBR (conversion levels greater than 97%) in a continuous process till date. In this work, a novel and successful continuous process (with Kenics® KMX SM as gas–liquid reactor) is designed, developed, and used for hydrogenation of NBR. The feasibility of the designed process, process conditions, and chemical parameters are studied by conducting hydrogenation experiments using the continuous process. The performance of the SM reactor is simulated by proposing a mechanistic model that takes into account the coupled behavior of reaction, flow, and mass transfer. Finally, the proposed model is validated with the experimental results.

## Experimental

### *Working fluids and reagents*

The working fluids used in the study are: NBR (Krynac 38.5 containing 62 wt % butadiene (80% trans, 15% cis, and 5% vinyl C=C) and 38 wt % acrylonitrile (AN) with a $M_n$ = 70,000 and a polydispersity of 3.6, was provided by LANXESS), osmium trichloride salt (supplied by Strem Chemicals), monochlorobenzene (supplied by Fisher Scientific), oxygen free nitrogen gas (supplied by Praxair), and hydrogen gas (99% pure, supplied by Praxair).

### *Synthesis of polymer solution*

The unsaturated polymer/rubber solution is prepared by dissolving the preweighed NBR in the solvent (monochlorobenzene). The concentration of the starting solution is adjusted such that the dilution due to the catalyst stream is compensated. Based on the polymer to catalyst flow ratio, higher concentration of rubber is used in the starting solution. The rubber to be dissolved in the solvent is cut into small pieces and transferred to a 20 L polyethylene carboy. The rubber is completely dissolved in the solvent by agitating with a mixer that has multiagitators (Rushton turbines) along the length of the rotating shaft. To overcome the problem of dissolved oxygen (because the rate of hydrogenation of NBR is hindered by the presence of oxygen in the system), the solution is degassed simultaneously with oxygen free nitrogen. The solution was then transferred into a 20 L polyethylene carboy. After that, again the solution is purged with oxygen free nitrogen through a dip tube for ~3–4 h before the actual experimental run is carried out. Thus, most care is taken to ensure that the solution will be almost free of oxygen/air.

### *Preparation of catalyst solution*

The catalyst used in this study is $OsHCl(CO)(O_2)(PCy_3)_2$. The catalyst is synthesized using the techniques described by Parent.[2] As the solid osmium catalyst is not air sensitive, it did not require any special storage. Nevertheless, when we use it in the form of solution in the continuous setup, it should be free of oxygen/air. The amount of catalyst required for the experiment is dissolved in a predetermined volume of degassed monochlorobenzene and transferred to a 1 L stainless steel bomb (supplied by Niagara Valve and Fittings Company, Canada), which is then pressurized with pure hydrogen and connected to the continuous reactor setup.

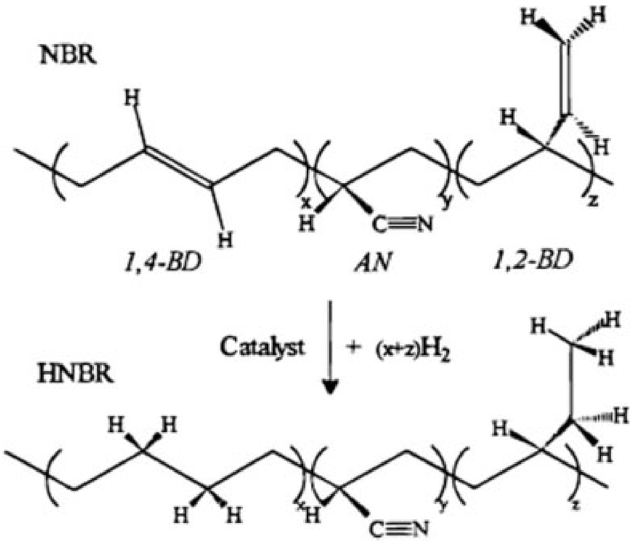

Figure 1. Scheme for hydrogenation of NBR.[2]

### *Hydrogenation kinetics*

Each butadiene (Bd) segment in NBR still contains a residual carbon–carbon double bond after the copolymerization of Bd and AN for making NBR. A cis- or trans-configuration of the polymer results when Bd polymerizes via 1,4-addition while a pendent vinyl bond is formed on a side chain if 1,2 addition occurs. The proportions of each of the configuration vary depending on the grade of NBR. For Krynac 38.50, the trans-configuration makes up ~75% of the unsaturation, whereas the vinyl bond accounts for only about 2%. The remnant olefinic bond in the polymer back bone causes a greater susceptibility to physical breakdown when exposed to heat, light, or ozone. By selectively hydrogenating these unsaturated bonds to form HNBR, the polymer's resistance to heat and ozone can be improved along with long durability when exposed to aggressive environments. Figure 1 shows the typical reaction scheme for hydrogenation of NBR. The osmium based catalyst, $OsHCl(CO)(O_2)(PCy_3)_2$ was found to be the most active catalyst compared with the Wilkinson's and ruthenium based catalysts.[2] The osmium catalyst is not stable in ketones and hence a chlorinated solvent is used. Also, unlike other catalysts, this catalyst does not require a cocatalyst to boost the activity. The osmium catalyst is also prone to crosslinking in NBR but to a much lesser extent than ruthenium catalysts. With the Wilkinson's catalyst and ruthenium catalysts, the reaction rate is generally first order with respect to the partial pressure of hydrogen. At high pressures and low-polymer concentration, it shifts to zero order. While with the osmium catalysts, a second-order dependence with respect to hydrogen pressure was observed up to a very high pressure before it goes to zero order. Hence, with the osmium catalyst, an increase in the reaction pressure would have a strong impact compared with Wilkinson's or ruthenium catalysts on the rate of hydrogenation. Hence, the rate of hydrogenation ($R_H$) with the osmium catalyst is given by Eq. 1.

$$R_H = k'[Os][C{=}C][H_2]^2 \tag{1}$$

where $k'$ is the reaction rate constant, [Os] is the osmium concentration, [C=C] is the double bond concentration in the NBR solution and [$H_2$] is the hydrogen concentration.

### *Experimental setup*

A bench scale continuous experimental setup was developed and constructed to conduct the hydrogenation of NBR. The experimental layout is shown in Figure 2.

The unsaturated polymer solution from the 20 L carboy (1) is pumped using the polymer-side pump (2, supplied by Milton Roy Company, Brampton, Canada) into the preheater (5). Before the preheater is filled with the unsaturated polymer solution, it is degassed with oxygen free hydrogen for half an hour. Oxygen free hydrogen is supplied from a compressed high-pressure cylinder and a mass flow controller (3, supplied by Brooks Company) is used to control/set the required flow of hydrogen. A distributing valve located after the mass flow controller is used to direct the flow either to the preheater or the SM reactor (9) or both depending on the required reactor operation conditions. The preheated unsaturated polymer solution and hydrogen gas mixture from the preheater enters the reactor through the three-way distribution valve (8) located at the bottom of the SM reactor. The distribution valve allows the reactor to be isolated from the transfer line and is also used to drain the reactor if necessary. The transfer line from the preheater to the reactor is insulated with fiber glass ribbon to avoid heat loss. Pure hydrogen gas enters the reactor through a gas sparger (18) located exactly opposite to the point where catalyst enters the reactor. The gas sparger has 15 holes of 1 mm diameter facing upwards.

The catalyst solution is pumped into the reactor using the catalyst side pump (7, supplied by Milton Roy Company, Brampton, Canada) at a predetermined flow rate. The desired catalyst concentration is achieved by adjusting the catalyst to polymer flow ratio. A three-way valve is located at the

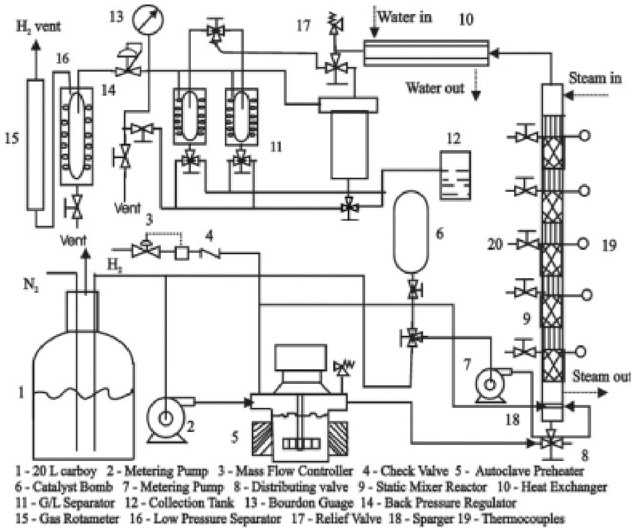

Figure 2. Schematic of the static mixer reactor setup used for hydrogenation of NBR.

bottom of the catalyst bomb which is used to purge the catalyst line to the reactor and for priming purposes in addition to pumping the catalyst solution. The hydrogen gas from the gas sparger and the catalyst stream enter the reactor in opposite directions and this ensures even distribution of catalyst in the unsaturated polymer solution at the entrance of the reactor. The SM reactor (9) is 123 cm long with 3.81 cm internal diameter (ID). The housing is made of 316 L stainless steel 80 schedule with 0.5 cm nominal wall thickness. Madhuranthakam et al.[5] showed that SM with 20 elements would give conversions over 95% under optimal conditions. With a safety design factor of 20%, the SM reactor had 24 Kenics® KMX mixing elements (supplied by Chemineer, MA) arranged such that the angle between neighboring elements is 90°. The reactor is surrounded with a 6.35 cm ID jacket through which steam flows. As the reaction is exothermic, most of the heat is released within the first half of the reactor while relatively less heat is released in the later section of the reactor. Hence, the steam flow in the jacket is operated in a countercurrent fashion with respect to the polymer flow in the reactor. The reactor jacket is wrapped with 1.9 cm thick fiber glass insulation to avoid heat loss to the environment. Sampling ports (20) were present at equal distance for every six elements (i.e., at 6th element, 12th element, 18th element, and 24th element). Exactly opposite to the other side of the sampling ports, thermocouples (19) are fixed which are in turn connected to a data acquisition system to record the temperatures online. The reacted polymer and the gas mixture from the reactor exits at the top and passes through a water cooled double pipe heat exchanger (10) operated in a counter current fashion. A three-way valve sequentially distributes the cooled gas–liquid mixture between a 2 L gas–liquid separator and two sight glasses (11, with 0.15 L volume) connected in parallel. The gas–liquid separation occurs by gravity, with the liquid settling at the bottom of the separator. The sight glasses are rated for 10.54 MPa and the 2 L separator is rated for 14 MPa. Although one of the separators is being filled with the reacted polymer solution, the other separator can be drained into a 12 L collection tank (12) via a three valve located at the bottom of each of the separators. Hydrogen gas exits at the top of the gas–liquid separators through an annular fitting and passes through a one-way check valve that isolates the separators while they are draining. A gas return line connected to the three-way valves at the bottom of the gas–liquid separators allows them to be repressurized after they have been drained of liquid. A Bourdon gauge (13) located after the check valve is used to measure the system pressure. The system pressure is controlled by using a back pressure regulator (14) rated to 10.54 MPa. A secondary sight glass (16) is located after the regulator to collect any residual liquid that might have been carried through as a result of a process upset. Finally, the exhaust hydrogen gas passes through a rotameter (15) and is vented to a stack.

### *FTIR analysis of NBR saturation*

The hydrogenation degree or the degree of saturation in the hydrogenated NBR samples is defined as:

$$\text{Hydrogenation Degree}(\%) = \frac{[\mathrm{C{=}C}]_0 - [\mathrm{C{=}C}]}{[\mathrm{C{=}C}]_0} \times 100 \quad (2)$$

where, $[\mathrm{C{=}C}]_0$ is the initial olefin concentration and $[\mathrm{C{=}C}]$ is the remaining olefin concentration. Fourier transform infrared spectroscopy (FTIR) is used to determine the exact concentration of the different olefin concentrations. The 2270 $\mathrm{cm}^{-1}$ peak resulting from the cyano group, the 970 $\mathrm{cm}^{-1}$ peak characteristic of the level of unsaturated transolefin by the proton vibration on the $\mathrm{C{=}C{-}H}$ and a modified peak at 730 $\mathrm{cm}^{-1}$, which resulted from the oscillating H attached to the saturated backbone $-\mathrm{CH_2}-\mathrm{CH_2}-$ are used to estimate the degree of hydrogenation according to the expression (Eq. 3) developed by Brück.[11]

$$\text{Degree of Hydrogenation}(\%) = \frac{\frac{A(730)}{k(730)}}{\left[A(2230) + \frac{A(970)}{k(970)} + \frac{A(730)}{k(730)}\right](1 - \mathrm{ACN})} \quad (3)$$

where $A(x)$ is the absorbance height at wavelength, $x$ $\mathrm{cm}^{-1}$, and ACN is the AN content in the rubber. The constants, $k(x)$, are determined by plotting the ratio $A(730)/A(2230)$ versus $A(970)/A(2230)$. More information is detailed in the work done by Parent.[2] Figure 3 shows a typical FTIR spectra obtained for the sample with 98.53% degree of hydrogenation.

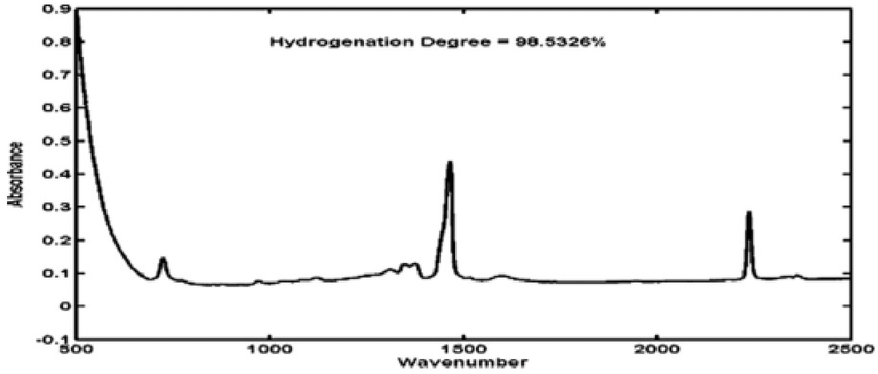

**Figure 3. Typical FTIR spectra obtained for rubber with 98.53% degree of hydrogenation.**

Table 1. List of the $2^3$ Experiments Conducted at 3.5 MPa and 138°C

| Experiment # | Mean Residence Time (min) | Polymer Conc. (mol/L) | Catalyst Conc. (mol/L) |
|---|---|---|---|
| 1 | 35.16 | 0.418 | $35 \times 10^{-6}$ |
| 2 | 35.16 | 0.418 | $80 \times 10^{-6}$ |
| 3 | 16.7 | 0.418 | $80 \times 10^{-6}$ |
| 4 | 16.7 | 0.418 | $120 \times 10^{-6}$ |
| 5 | 35.18 | 0.837 | $100 \times 10^{-6}$ |
| 6 | 35.18 | 0.837 | $130 \times 10^{-6}$ |
| 7 | 17.0 | 0.837 | $85 \times 10^{-6}$ |
| 8 | 17.0 | 0.837 | $140 \times 10^{-6}$ |

## Results and Discussion

### *Experimental results*

Hydrogenation experiments were conducted in the bench scale continuous setup with different operating conditions to evaluate the performance of the SM reactor. Experiments were designed such that the pressure is maintained at 3.5 MPa and the temperature was targeted to be 138°C. From the batch experimental results conducted by Parent,[2] it was evident that the catalyst activity increases with the increase in the reaction temperature while an increase in pressure also had a proportional effect on the degree of hydrogenation. Hence, keeping the pressure and the temperature constant, other operating parameters such as, the polymer concentration, the catalyst concentration, and the mean residence time were varied to study the performance of the SM reactor. It is observed that the gas flow rate has a significant effect on the performance of the SM reactor. One of the most important design parameters that has a strong impact on the performance of the SM reactor is the gas hold up, which in turn depends on the gas–liquid flow rates. Although at a lower gas hold up, the turn over of the hydrogenated polymer is greater, yet the degree of hydrogenation may be lower because of the lower availability of hydrogen in the liquid phase. On the other hand, a high gas hold up could reduce the residence time of the polymer solution in the reactor, which also could decrease the hydrogenation degree. Hence, there lies an optimal liquid hold up for achieving higher turn over with a good degree of hydrogenation. From the hydrodynamic experimental results done by Madhuranthakam,[12] it was observed that ~90% liquid hold up can be obtained when the superficial gas flow rate is four to six times of the superficial polymer flow rate. A $2^3$ factorial experiments were designed and performed with the factors being polymer concentration, catalyst concentration, and mean residence time at two levels. The two levels in the polymer concentration are 0.418 and 0.837 mol/L, whereas for the mean residence time they are 16 and 36 min. The two levels of the catalyst concentration were fixed based on the degree of hydrogenation obtained with the low level catalyst and taking the catalyst deactivation into consideration.

Table 1 shows the factorial experiments performed in the SM reactor to study the effect of different operating parameters on the degree of hydrogenation. For the experiments in which the mean residence time was 35 min, the hydrogen flow rate was six times that of the polymer flow rate, whereas it was four times of the polymer flow rate for the experiments in which the residence time experiments was 17 min.

Figure 4 shows the comparison of the steady state degree of hydrogenation obtained for the two replicate runs performed in the continuous process where the polymer concentration is 0.418 mol/L, the catalyst concentration is $80 \times 10^{-6}$ mol/L and the mean residence time is 35.16 min. From statistical analysis, the mean square error in the degree of hydrogenation from these replicate runs is found to be ±0.866%. This error is used in the statistical analysis (discussed in the later section). The hydrogenation experiments were performed such that the catalyst concentration level is initially at a low level. Based on the degree of hydrogenation, the catalyst concentration is increased in steps of 50–100%. The desired catalyst concentration is the minimum catalyst concentration required to obtain at least a 95% degree of hydrogenation for a given polymer concentration and mean residence time.

Figure 5 shows the dynamic profiles of degree of hydrogenation versus time obtained after 6 elements, 12 elements, 18 elements, and 24 elements for the experiment with 0.418 mol/L polymer concentration, $80 \times 10^{-6}$ mol/L catalyst concentration and 35.16 min mean residence time. Figure 6 shows the corresponding reaction temperature profiles versus time (for the same experiment as shown in Figure 5). In this experiment, the maximum conversion achieved at the end of 24 elements is ~98%. The profiles are fairly smooth and steady state is reached after 108 min which is approximately three times of the mean residence time ($\tau = 35.16$ min). The same experiment with the catalyst concentration being $35 \times 10^{-6}$ mol/L yielded a maximum of 74% degree of hydrogenation. From Figure 6, it is evident that almost uniform temperature is maintained along the length of the reactor. It is observed that in all experiments, the temperature at the inlet of the reactor was 6–8°C lower than the design temperature.

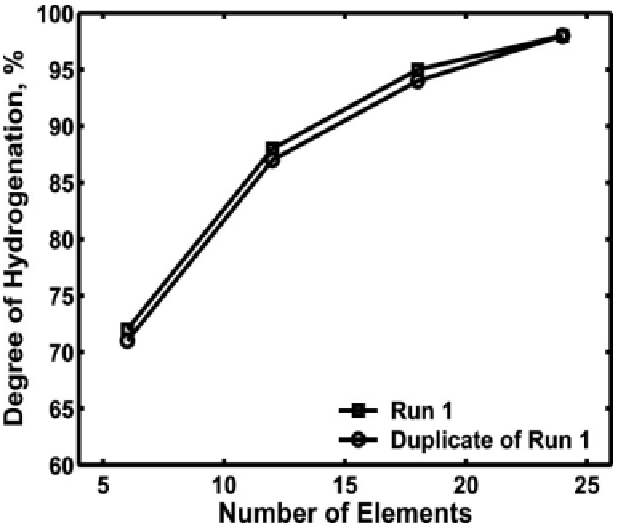

**Figure 4. Comparison of steady state conversions obtained in the SM reactor for experiments with identical operating conditions ($C_{poly}$ = 0.418 mol/L, $C_{cat}$ = $80 \times 10^{-6}$ mol/L, $\tau$ = 35.16 min, $Q_{pol}$ = 24 cm$^3$/min, $Q_{H_2}$ = 144 cm$^3$/min, $Q_{cat}$:$Q_{pol}$ = 1:5).**

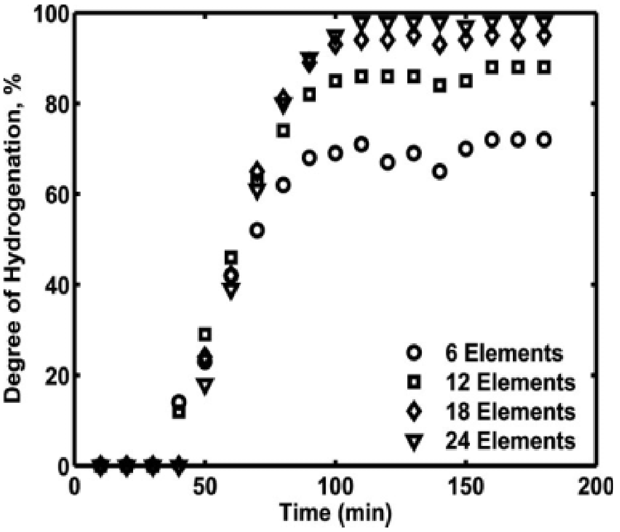

Figure 5. Degree of hydrogenation versus time (operating conditions: $C_{poly}$ = 0.418 mol/L, $C_{cat}$ = 80 × $10^{-6}$ mol/L, $\tau$ = 35.16 min, $Q_{pol}$ = 24 $cm^3$/min, $Q_{H_2}$ = 144 $cm^3$/min, $Q_{cat}$:$Q_{pol}$ = 1:5).

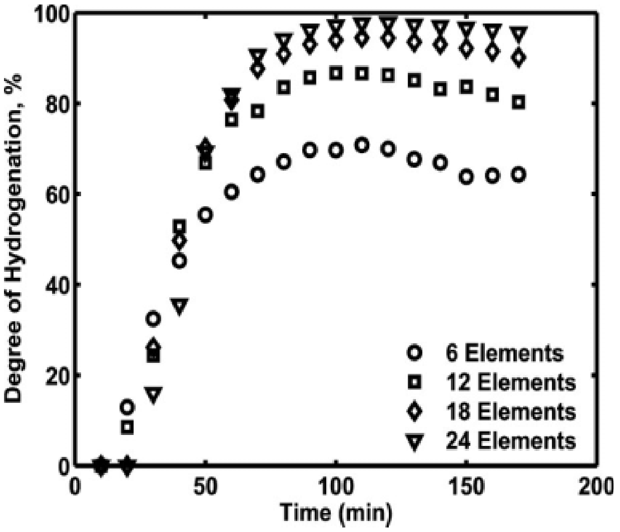

Figure 7. Degree of hydrogenation versus time (operating conditions: $C_{poly}$ = 0.837 mol/L, $C_{cat}$ = 130 × $10^{-6}$ mol/L, $\tau$ = 35.18 min, $Q_{pol}$ = 23 $cm^3$/min, $Q_{H_2}$ = 144 $cm^3$/min, $Q_{cat}$:$Q_{pol}$ = 1:5).

This is due to the fact that cold catalyst solution enters as a separate stream at the inlet of the reactor. Before conducting the designed experiments (refer Table 1) with the 0.837 mol/L polymer system, two experiments were performed with very low catalyst concentration for both low and high levels of the mean residence time. Severe catalyst deactivation was witnessed in both the experiments. The degree of hydrogenation with $\tau$ = 35.18 min, 60 × $10^{-6}$ mol/L catalyst was 43.5% and with $\tau$ = 35.18 min, 85 × $10^{-6}$ mol/L catalyst it was 52.7%. There are three possible reasons to explain the catalyst deactivation phenomenon. One of them is, when the polymer concentration is increased the concentration of the impurities in the polymer also increases which reduces the reaction rate.

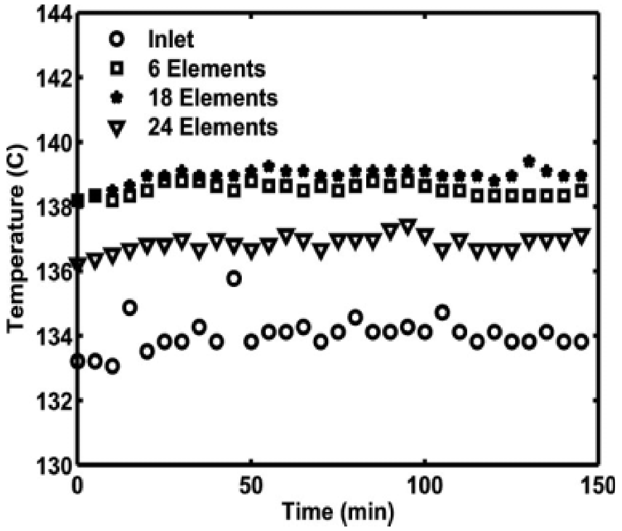

Figure 6. Temperature versus time (operating conditions: $C_{poly}$ = 0.418 mol/L, $C_{cat}$ = 80 × $10^{-6}$ mol/L, $\tau$ = 35.16 min, $Q_{pol}$ = 24 $cm^3$/min, $Q_{H_2}$ = 144 $cm^3$/min, $Q_{cat}$:$Q_{pol}$ = 1:5).

The next reason could be inefficient degassing and susceptibility of air in the reactor mixture. The last but most important reason is, though the double bond concentration ([C=C]) does not have an effect on the reaction rate constant, the nitrile concentration has a significant impact on the reaction rate. This is due to the tendency of the catalyst to coordinate to the cyano group.[2] The cyano group in the NBR (refer Figure 1) competes with the double bond to occupy the catalytic sites and thereby hinders the reaction rate. A further experiment was performed with the catalyst concentration maintained at 100 × $10^{-6}$ mol/L for $\tau$ = 36 min and the maximum steady state conversion achieved at the exit of the SM reactor is 82.63%. Hence, experiments 7 and 8 (refer Table 1) were designed and performed to achieve a degree of hydrogenation over 95% despite catalyst deactivation. Figures 7 and 8 show the degree of hydrogenation profiles obtained for experiments 7 and 8 carried out with a 0.837 mol/L polymer system where a degree of hydrogenation of over 97% was achieved in both cases. From the factorial experiments, the following desired catalyst concentrations (refer Table 2) are obtained for an objective of getting over 97% degree of hydrogenation.

The final conversions (at steady state) obtained from the hydrogenation experiments tended to follow the expected first-order profiles. The corresponding reaction rate constants ($k'$) were determined by plotting ln(1-conversion) versus reaction time and calculating the slope.

### *Statistical analysis*

From the experimental results obtained from the designed $2^3$ factorial experiments (refer Table 1), statistical analysis was performed to evaluate the effect of different factors considered. As mentioned earlier, the error from the replicated runs is used for analysis of the variance. Table 3 shows the

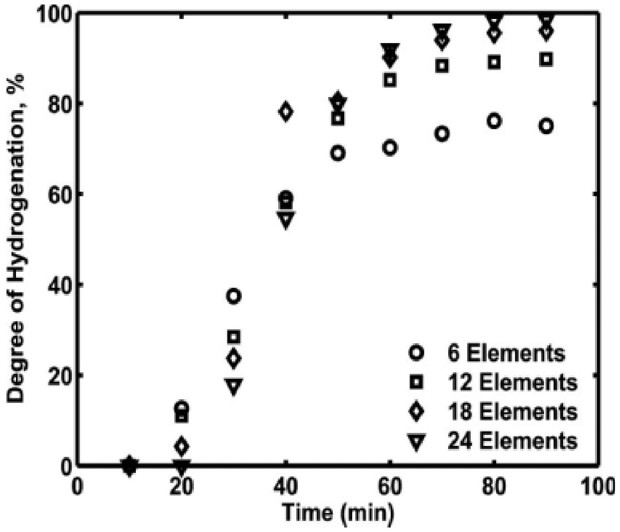

**Figure 8. Degree of hydrogenation versus time (operating conditions: $C_{poly} = 0.837$ mol/L, $C_{cat} = 140 \times 10^{-6}$ mol/L, $\tau = 17$ min, $Q_{pol} = 40$ cm$^3$/min, $Q_{H_2} = 200$ cm$^3$/min, $Q_{cat}:Q_{pol} = 1:4$).**

coded variables corresponding to the experiments listed in Table 1. In Table 3, A, B, and C are the coded variables for catalyst concentration, mean residence time, and polymer concentration, respectively.

Table 4 shows the analysis of variance corresponding to the experiments listed in Table 3. The analysis was carried out with a significance level of 0.05. In Table 4, S specifies that the results are significant, whereas NS specifies not significant. The analysis clearly shows that the factors chosen to study the degree of hydrogenation have a strong impact. The first-order effects and second-order interactions are found to be significant, whereas the third-order interactions were not significant.

### *Mechanistic model*

The performance of the SM reactor with respect to hydrogenation of NBR is simulated and numerically analyzed by proposing a mechanistic model that takes flow, reaction, and mass transfer phenomenon into consideration. For derivation of the model, refer the Appendix section. The knowledge about the residence time distribution (RTD) in SMs is very important when the mixer is used as a chemical reactor.[13] The RTD in a SM with open blade internal structure under laminar flow condition can be described by using Danckwerts' axial dispersion model.[14] By incorporating the RTD, hydrogenation reaction kinetics and mass transfer of hydrogen gas to the unsaturated polymer solution, the following model (described by Eq. 4–6) is derived for conversion, hydrogen concentration in the polymer phase and catalyst concentration (in dimensionless form).

**Table 2. Desired Catalyst Concentration Obtained from Factorial Experiments**

| Desired Catalyst Concentration (mol/L) | Polymer Concentration (mol/L) | Mean Residence Time (min) |
|---|---|---|
| $80 \times 10^{-6}$ | 0.418 | 35.18 |
| $120 \times 10^{-6}$ | 0.418 | 16.7 |
| $130 \times 10^{-6}$ | 0.837 | 35.16 |
| $140 \times 10^{-6}$ | 0.837 | 17 |

**Table 3. Coded Variables and Corresponding Conversions for the $2^3$ Experiments**

| Factor-Level Combination | | | Conversion (%) Replicates | |
|---|---|---|---|---|
| A | B | C | | |
| 1 | 1 | 1 | 84.97 | 85.84 |
| 2 | 1 | 1 | 97.65 | 98.52 |
| 1 | 2 | 1 | 73.88 | 74.75 |
| 2 | 2 | 1 | 82.63 | 83.50 |
| 1 | 1 | 2 | 97.06 | 97.93 |
| 2 | 1 | 2 | 99.95 | 99.08 |
| 1 | 2 | 2 | 98.00 | 98.87 |
| 2 | 2 | 2 | 96.40 | 97.27 |

1, represents the lower level; 2, represents the higher level of the factor.

$$\frac{\partial x}{\partial \theta} = \frac{1}{Pe} \cdot \frac{1}{\theta_\tau} \frac{\partial^2 x}{\partial \lambda^2} - \frac{1}{\theta_\tau} \frac{\partial x}{\partial \lambda} + (1 - x) \cdot \zeta \cdot h^2 \tag{4}$$

$$\frac{\partial h}{\partial \theta} = \frac{1}{Pe} \cdot \frac{1}{\theta_\tau} \frac{\partial^2 h}{\partial \lambda^2} - \frac{1}{\theta_\tau} \frac{\partial h}{\partial \lambda} - q \cdot (1 - x) \cdot \zeta \cdot h^2 + \frac{q}{R}(1 - h) \tag{5}$$

$$\frac{\partial \zeta}{\partial \theta} = \frac{1}{Pe} \frac{1}{\theta_\tau} \frac{\partial^2 \zeta}{\partial \lambda^2} - \frac{1}{\theta_\tau} \frac{\partial \zeta}{\partial \lambda} \tag{6}$$

The corresponding open–open boundary conditions are given by the following equations.

$$\text{Initial Condition: At} \quad \theta = 0;\ \forall \lambda \quad x = 0, \quad h = h_0, \quad \zeta = 0$$

$$\text{Boundary Condition 1:}$$

$$\text{At} \quad \lambda = 0; \quad \upsilon(0^-, \theta) + \frac{1}{Pe} \frac{\partial \upsilon}{\partial \lambda}\bigg|_{(0^-,\theta)} = \upsilon(0^+, \theta) + \frac{1}{Pe} \frac{\partial \upsilon}{\partial \lambda}\bigg|_{(0^+,\theta)}$$
$$\upsilon(0^-, \theta) = \upsilon(0^+, \theta)$$

$$\text{Boundary Condition 2:}$$

$$\text{At} \quad \lambda = 1; \quad \upsilon(1^-, \theta) + \frac{1}{Pe} \frac{\partial \upsilon}{\partial \lambda}\bigg|_{(1^-,\theta)} = \upsilon(1^+, \theta) + \frac{1}{Pe} \frac{\partial \upsilon}{\partial \lambda}\bigg|_{(1^+,\theta)}$$
$$\upsilon(1^-, \theta) = \upsilon(1^+, \theta)$$

$$\text{where,} \quad \upsilon = x, h, \zeta$$

In the aforementioned equations, $Pe$ is the Peclet number defined as $Pe = \frac{\overline{U}L}{D_a}$, $x$ is the conversion, $h$ is the normalized hydrogen concentration, $\zeta$ is the normalized catalyst concentration, $\theta$ is the dimensionless time ($t/\tau$), and $\lambda$ is the dimensionless length ($z/L$). For definitions of $R$, $q$, and $\theta_\tau$, refer the Appendix section. The important parameters required to solve the aforementioned model are $Pe$, $R$, $q$, and $\theta_\tau$. Peclet number in the Kenics® KMX SM with the similar system of experimental fluids (hydrogen gas and polymer solution) has been modeled by Madhuranthakam[12] as function of liquid-

Table 4. Analysis of Variance for the Experiments Listed in Table 3

| V | SS | df | MS | F | P | Conclusion |
|---|---|---|---|---|---|---|
| Model | 1247.2381 | 7 | | | | |
| A | 119.3993 | 1 | 119.3993 | 318.4169 | 0.0000 | S |
| B | 193.9613 | 1 | 193.9613 | 517.2606 | 0.0000 | S |
| C | 660.8498 | 1 | 660.8498 | 1762.3697 | 0.0000 | S |
| AB | 14.2657 | 1 | 14.2657 | 38.0442 | 0.0003 | S |
| AC | 110.3130 | 1 | 110.3130 | 294.1853 | 0.0000 | S |
| BC | 148.4255 | 1 | 148.4255 | 395.8245 | 0.0000 | S |
| ABC | 0.0234 | 1 | 0.0234 | 0.0624 | 0.8090 | NS |
| Error | 2.9998 | 8 | 0.3750 | | | |
| Total | 1250.2380 | 15 | | | | |

side and gas-side hydraulic Reynolds numbers. The empirical model is given by:

$$Pe = \beta_1 Re_{L-h}^{\beta_2} Re_{G-h}^{\beta_3} \tag{7}$$

where $\beta_1$, $\beta_2$, and $\beta_3$ are constants, $Re_{\text{L-h}}$ and $Re_{\text{G-h}}$ are Reynolds numbers defined based on the hydraulic mean diameter ($D_H$) of the SM reactor. There is very scant literature on the mass transfer coefficient in the SM reactor with the polymer system. Nevertheless, the mass transfer coefficient in a similar reactor with flat blade internal structure (Sulzer® SMX) with air water system is empirically modeled as a function of liquid-side and gas-side Reynolds numbers by Madhuranthakam et al.[15] As an approximation, the mass transfer coefficient $K_La$, is estimated from the correlation given by them (Eq. 8).

$$K_La = \text{A}N_{\text{Re}_\text{L}}^{\alpha} N_{\text{Re}_\text{G}}^{\beta} \tag{8}$$

where $A$, $\alpha$, and $\beta$ are constants, $N_{\text{Re}_\text{L}}$ and $N_{\text{Re}_\text{G}}$ are liquid-side and gas-side Reynolds numbers. Finally, the reaction rate constant ($k'$) is evaluated from the final conversions obtained in the SM reactor by plotting $\ln(1 - x_{\text{final}})$ versus time. With the aforementioned information, all the parameters of the model ($Pe$, $R$, $q$, and $\theta_\tau$) are evaluated. The proposed model contains coupled, nonlinear partial differential equations. As this is an initial boundary value problem (IBVP), method of lines (MOL) is conveniently used to solve for the conversion (or degree of hydrogenation). This is realized by a two-step procedure. First, the spatial derivatives on the right side of the design equations are replaced by numerical approximation using finite differences. The resulting equations would be ordinary differential equations which are continuous in time. Finally, they are solved by using MATLAB ODE stiff solvers.

Figures 9 and 10 show a comparison of the experimental degree of hydrogenation with the proposed model prediction for typical hydrogenation experiments conducted in the continuous process with the SM reactor. In Figure 9 and 10, the parameters of the proposed model are obtained from the corresponding equations defined in Appendix section. Table 5

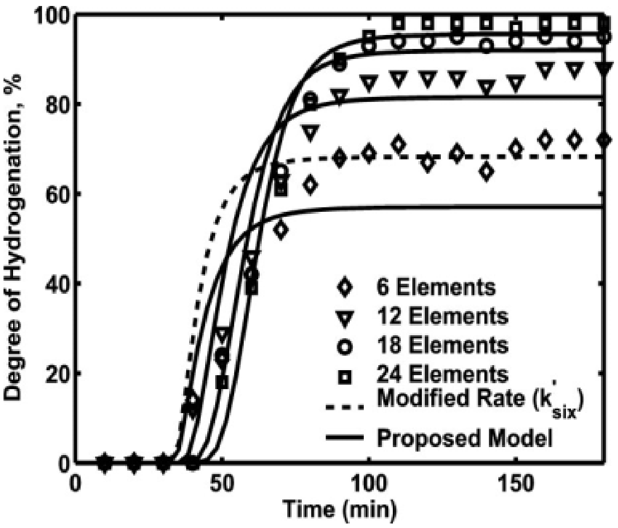

**Figure 9.** Model prediction versus experimental degree of hydrogenation (operating conditions: $C_{\text{poly}}$ = 0.418 mol/L, $C_{\text{cat}}$ = 80 × $10^{-6}$ mol/L, $\tau$ = 35.16 min, $Q_{\text{pol}}$ = 24 cm$^3$/min, $Q_{H_2}$ = 144 cm$^3$/min, $Q_{\text{cat}}$:$Q_{\text{pol}}$ = 1:5, parameters of the model: Pe = 8.26, $\theta_\tau$ = 4.77, $R$ = 1.8, $q$ = 0.00247).

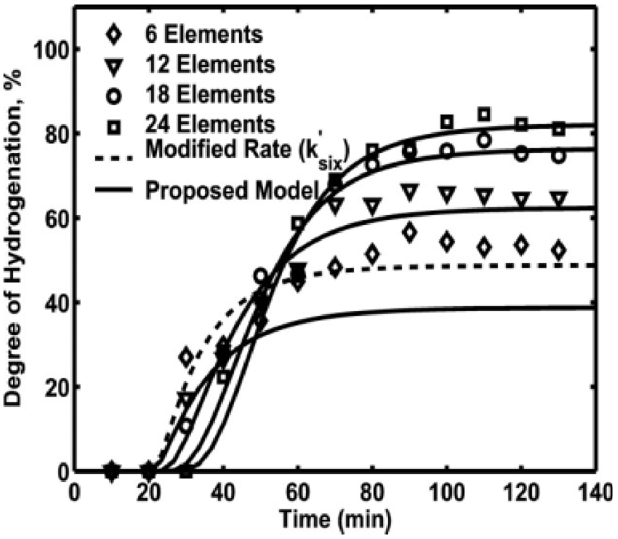

**Figure 10.** Model prediction versus experimental degree of hydrogenation (operating conditions: $C_{\text{poly}}$ = 0.837 mol/L, $C_{\text{cat}}$ = 100 × $10^{-6}$ mol/L, $\tau$ = 35.16 min, $Q_{\text{pol}}$ = 23 cm$^3$/min, $Q_{H_2}$ = 144 cm$^3$/min, $Q_{\text{cat}}$:$Q_{\text{pol}}$ = 1:5, parameters of the model: Pe = 5.33, $\theta_\tau$ = 2.69, $R$ = 1.6, $q$ = 0.00494).

Table 5. Parameters and Constants Used in the Simulation of Proposed Model

| Physical Quantity | $[C{=}C]_0$ = 0.418 (mol/L) | $[C{=}C]_0$ = 0.837 (mol/L) | Notes |
|---|---|---|---|
| $\rho_L$ (kg/m$^3$)$^{16}$ | 1163 | 1166 | at 25°C |
| $\mu_L$ (Pa s)$^{16}$ | 0.0739 | 0.1613 | at 25°C |
| $Re_{G\text{-}h}$ | 8.622 | 8.622 | $\frac{D_h \overline{U}_g \rho_g}{\mu_g}$ |
| $Re_{L\text{-}h}$ | 0.1 | 0.4 | $\frac{D_h \overline{U}_L \rho_L}{\mu_L}$ |
| $N_{Re_G}$ | 20.47 | 20.47 | $\frac{D \overline{U}_g \rho_g}{\mu_g}$ |
| $N_{Re_L}$ | 0.21 | 0.95 | $\frac{D \overline{U}_L \rho_L}{\mu_L}$ |
| $k_L a$, (s$^{-1}$)$^{16}$ | $2.46 \times 10^{-3}$ s$^{-1}$ | $2.74 \times 10^{-3}$ s$^{-1}$ | Eq. 8 |
| $K'$, s$^{-1}$ | 0.0017 | 0.0009 | at 138°C |
| $\theta_\tau$ | 4.77 | 2.685 | Eq. A7 |
| $Pe^{13}$ | 8.26 | 5.33 | Eq. 7 |
| $q$ | 0.00247 | 0.00494 | Eq. A8 |
| $R$ | 1.8 | 1.6 | Eq. A10 |
| [H*] (mmol/L)$^2$ | 169.11 (at 138°C, 3.5 MPa) | | |
| $\rho_g$ (kg/m$^3$) | 2.901 (at 25°C) | | |
| $\mu_g$ (Pa s) | $11.185 \times 10^{-6}$ (at 25°C) | | |
| $D_h$, cm | 1.64 | | |

shows the model parameters used and/or obtained for the corresponding experimental results shown in Figures 9 and 10.

All hydrogenation results were fit similarly with the proposed model, it is evident from the results that the proposed model satisfactorily predicts the degree of hydrogenation obtained from experimental results. However, the model could not predict correctly the degree of hydrogenation at six elements in all the cases. This is due to the higher reaction rate when osmium catalyst is used for hydrogenation of NBR solution compared with the Wilkinson's catalyst or the ruthenium catalysts. The rate of hydrogenation is usually very high during the first 25% of the reaction, which is due to the facile hydrogenation of cis- and vinyl-olefin (refer Figure 1), whereas the remaining reaction time is spent hydrogenating the transolefin at a much slower rate. This phenomenon is observed and validated by Parent[2] in the experiments done in a batch reactor. The same phenomenon is also observed in all experiments performed in the continuous reactor setup. Owing to this fact of higher reaction rate for the first 25% of the reaction, the modified rate constant ($k'_{six}$ which is 50% greater than the actual rate constant) is used in the proposed model to predict the degree of hydrogenation at the six elements. The corresponding performance of the model at six elements is shown in Figures 9 and 10 by the dotted line. It clearly shows that when the modified rate constant is used, the proposed model prediction at six elements is in good agreement with the experimental results. Similar trends were obtained from the model for all the experimental results. Overall, the proposed mechanistic model could predict the trends and approximate degree of hydrogenation in the SM reactor for various operating conditions.

## Conclusions

A continuous reactor setup has been developed for efficient production of hydrogenated NBR using homogeneous catalyst. For the first time, a Kenics® KMX SM reactor is designed to serve as the gas–liquid reactor in the continuous process. Successful hydrogenation (over 97% degree of hydrogenation) was obtained for different operating conditions. The optimum amount of catalyst to be used for achieving a degree of hydrogenation above 95% is proposed. A mechanistic model was proposed for evaluating the performance of the SM reactor numerically and is validated with the corresponding experimental results.

## Acknowledgements

This work was supported by the Natural Sciences and Engineering Research Council of Canada (NSERC) and LANXESS.

## Notation

$A$ = area of the reactor ($\pi D^2/4$, cm$^2$)
A, B, C = code variables
$C$ = concentration (mol L$^{-1}$)
$D$ = diameter of the reactor
$D_a$ = axial dispersion coefficient (m$^2$/s)
$D_h$ = hydraulic mean diameter (cm)
$h$ = dimensionless variable (normalized hydrogen concentration)
$k'$ = reaction rate constant
$K_L a$ = over all mass transfer coefficient (s$^{-1}$)
$M_n$ = number average molecular weight
$N_{Re_G}$ = gas-side Reynolds number
$N_{Re_L}$ = liquid-side Reynolds number
Os = osmium
$Pe$ = Peclet number
$q$ = dimensionless variable
$Q$ = flow rate (cc/min)
$Re$ = Reynolds number
$Re_{G\text{-}h}$ = gas-side hydraulic Reynolds number
$Re_{L\text{-}h}$ = liquid-side hydraulic Reynolds number
$R$ = dimensionless variable
$R_H$ = hydrogenation reaction rate (mol s$^{-1}$)
$t$ = time (s)
$\overline{U}$ = average velocity ($Q$*$A$, cm s$^{-1}$)
$V$ = variable
$x$ = conversion w.r.t double bond concentration
$y$ = arbitrary dependent variable
$z$ = variable representing reactor length (m)
[Os] = concentration of osmium
[H$_2$] = concentration of hydrogen
[C=C] = concentration of double bond

### Greek letters

$\beta$ = constant
$\rho$ = density (kg/m$^3$)
$\mu$ = viscosity (Pa s)
$\tau$ = space time (s)
$\theta$ = dimensionless time ($t/\tau_R$)
$\lambda$ = dimensionless reactor length ($z/L$)
$\zeta$ = normalized catalyst concentration
$\upsilon$ = variable (representing $x$, $h$, or $\zeta$)

### Subscripts

a = axial
cat = catalyst
g = gaseous phase (hydrogen/air)
g-h = gas-side hydraulic
L = liquid phase (polymer solution/water)
L-h = liquid-side hydraulic
0 = initial
poly = polymer
R = based on reaction only
six = after the six element

### Superscripts

$*$ = equilibrium value
$-$ = left neighborhood
$+$ = right neighborhood

### Abbreviations

AN = acrylonitrile
Bd = butadiene
Conc. = concentration
CSTR = continuously stirred tank reactor
df = degrees of freedom
ID = inside diameter
MCB = monochlorobenzene
MS = mean squares
NS = not significant
PFR = plug flow reactor
S = significant
SM = static mixer
SS = sum of squares
RTD = residence time distribution

## Literature Cited

1. Rempel GL. Catalytic hydrogenation of nitrile butadiene rubber. *Polym Prepr*. 2000;41:1507–1508.
2. Parent JS. Catalytic Hydrogenation of Butadiene Copolymers, *Ph.D. Thesis*. Waterloo, ON, Canada: University of Waterloo, 1996.
3. Kehl S. Catalytic Hydrogenation of Nitrile Butadiene Rubber in a Packed Bed, *M.A.Sc. Thesis*. Waterloo, ON, Canada: University of Waterloo, 1998.
4. Pan Q, Rempel GL, Ng FTT. Numerical investigation of continuous processes for catalytic hydrogenation of nitrile butadiene rubber. *Polym Eng Sci*. 2002;42:899–910.
5. Madhuranthakam CR, Pan Q, Rempel GL. Numerical investigation and experimental validation of the performance of a tubular packed bed reactor for hydrogenation of diene-based polymers, *Polym. Eng. Sci*. 2009;49(10):1979–1989.
6. Baker JR. Motionless mixers stir up new uses. *Chem Eng Prog*. 1991;87:32–38.
7. Cybulski A. Werner K. Static mixers—criteria for applications and selection. *Int Chem Eng*. 1986;26:171–180.
8. Myers KJ, Bakker A, Ryan D. Avoid agitation by selecting static mixers. *Chem Eng Prog*. 1997;6:28–38.
9. Thakur KJ, Vial Ch, Nigam KDP, Nauman EB, and Djelveh G. Static mixers in the process industries—a review. *Trans IChemE*. 2003;81:787–826.
10. Heniche M, Tanguy PA, Reeder MF, Fasano JB. Numerical investigation of blade shape in static mixing. *AIChE J*. 2005;51:44–58.
11. Brück D. IR-spectrometric determination of the proportions of acrylonitril, butadiene and hydrogenated butadiene in hydrogenated acrylonitrile-butadiene rubbers. I. Principles. *Kautschuk Gummi Kunststoffe*. 1989;42:107–110.
12. Madhuranthakam CR. Design, Modeling and Analysis of a Continuous Process for Hydrogenation of Diene Based Polymers Using a Static Mixer Reactor, *Ph.D. Thesis*. Waterloo, ON, Canada: University of Waterloo, 2007.
13. Streiff FA, Rogers JA. Don't overlook static mixer reactors. *Chem Eng J*. 1994;6:76–82.
14. Danckwerts PV. Continuous flow systems. *Chem Eng Sci*. 1953;2:1–13.
15. Madhuranthakam CR, Pan Q, Rempel GL. Hydrodynamics in sulzer SMX static mixer with air/water system. *Ind Eng Chem Res*. 2009;48:719–726.
16. Pan Q, Rempel GL. Investigation of fundamental data for nitrile butadiene rubber in monochlorobenzene and *O*-dichlorobenzene. *Polym Eng Sci*. 2004;44:88–95.

## Appendix

The Danckwert's dispersion model[14] superimposed with hydrogenation reaction rate and mass transfer applied to the concentrations of carbon–carbon double bond (C=C), hydrogen gas in the polymer, osmium catalyst for a differential section of the SM reactor are given by Eqs. A1–A3, respectively.

$$\frac{\partial[\mathrm{C{=}C}]}{\partial t} = D_\mathrm{a}\frac{\partial^2[\mathrm{C{=}C}]}{\partial z^2} - \overline{U}\frac{\partial[\mathrm{C{=}C}]}{\partial z} - R_\mathrm{H} \tag{A1}$$

$$\frac{\partial[\mathrm{H_2}]}{\partial t} = D_\mathrm{a}\frac{\partial^2[\mathrm{H_2}]}{\partial z^2} - \overline{U}\frac{\partial[\mathrm{H_2}]}{\partial z} - R_\mathrm{H} + K_\mathrm{L}a\left(\left[\mathrm{H_2^*}\right] - [\mathrm{H_2}]\right) \tag{A2}$$

$$\frac{\partial[\mathrm{O}s]}{\partial t} = D_\mathrm{a}\frac{\partial^2[\mathrm{O}s]}{\partial z^2} - \overline{U}\frac{\partial[\mathrm{O}s]}{\partial z} \tag{A3}$$

where [C=C] is the double bond concentration, $[H_2]$ is the hydrogen concentration, and $[H_2*]$ is the equilibrium concentration of hydrogen, $t$ is time, $z$ is the differential length of the reactor, $\overline{U}$ is the average velocity, $R_H$ is the hydrogenation reaction rate, [Os] is the osmium concentration, $D_a$ is axial dispersion coefficient and $K_La$ is the overall mass transfer coefficient. As the gas phase is pure hydrogen, the mass transfer in the gas phase and in the film are assumed to be negligible. Hence, the overall mass transfer is equal to the liquid side mass transfer coefficient which in turn depends on the geometry and type of packing, properties of the reactants, and operating conditions. The assumptions made in deriving the aforementioned model are: (i) the film model for mass transfer is valid and the extent of reaction in the liquid film is negligible; (ii) the temperature and the pressure are steady and constant; (iii) the mass transfer coefficient and the interfacial area are constant; (iv) the axial dispersion ($D_a$) is independent of concentration and position; and (v) the reaction takes place in the bulk of the polymer solution and there is almost negligible reaction in the gas phase alone. The hydrogenation reaction rate when osmium is used as catalyst is given by Eq. A4.[2]

$$R_\mathrm{H} = k'[\mathrm{O}s][\mathrm{C{=}C}][\mathrm{H_2}]^2 \tag{A4}$$

To study the effect of different important factors that affect the degree of hydrogenation in the SM reactor, the aforementioned equations are converted into dimensionless form using the dimensionless variables defined as follows:

$$\lambda = \frac{z}{L} \tag{A5}$$

$$\theta = \frac{t}{\tau_\mathrm{R}} \tag{A6}$$

$$\theta_\tau = \frac{\tau}{\tau_\mathrm{R}} \tag{A7}$$

$$q = \frac{[\mathrm{C{=}C}]_0}{[\mathrm{H_2}]} \tag{A8}$$

$$\tau_\mathrm{R} = \frac{1}{k'[\mathrm{Os}]_0\left[\mathrm{H_2^*}\right]^2} \tag{A9}$$

$$R = \frac{k'[\mathrm{C{=}C}]_0[\mathrm{Os}]_0\left[\mathrm{H}_2^*\right]^2}{K_\mathrm{L}a\left[H_2^*\right]} \tag{A10}$$

$$\tau = \frac{L}{\overline{U}} \tag{A11}$$

$$x = 1 - \frac{[\mathrm{C{=}C}]}{[\mathrm{C{=}C}]_0} \tag{A12}$$

$$h = \frac{[\mathrm{H}_2]}{\left[\mathrm{H}_2^*\right]} \tag{A13}$$

$$\zeta = \frac{[\mathrm{Os}]}{[\mathrm{Os}_0]} \tag{A14}$$

With the aforementioned variables substituted in Eqs. A1–A3, the resulting model in the dimensionless form is given the following equations:

$$\frac{\partial x}{\partial \theta} = \frac{1}{Pe}\cdot\frac{1}{\theta_\tau}\frac{\partial^2 x}{\partial \lambda^2} - \frac{1}{\theta_\tau}\frac{\partial x}{\partial \lambda} + (1-x)\cdot\zeta\cdot h^2 \tag{A15}$$

$$\frac{\partial h}{\partial \theta} = \frac{1}{Pe}\cdot\frac{1}{\theta_\tau}\frac{\partial^2 h}{\partial \lambda^2} - \frac{1}{\theta_\tau}\frac{\partial h}{\partial \lambda} - q\cdot(1-x)\cdot\zeta\cdot h^2 + \frac{q}{R}(1-h) \tag{A16}$$

$$\frac{\partial \zeta}{\partial \theta} = \frac{1}{Pe}\frac{1}{\theta_\tau}\frac{\partial^2 \zeta}{\partial \lambda^2} - \frac{1}{\theta_\tau}\frac{\partial \zeta}{\partial \lambda} \tag{A17}$$

The corresponding open–open boundary conditions in the dimensionless form are given as follows:

$$\begin{aligned}
&\text{Initial Condition: At}\quad \theta = 0;\ \forall\lambda\quad x = 0,\quad h = h_0,\quad \zeta = 0\\
&\text{Boundary Condition 1 :}\\
&\text{At}\quad \lambda = 0;\quad \upsilon(0^-,\theta) + \frac{1}{Pe}\frac{\partial \upsilon}{\partial \lambda}\bigg|_{(0^-,\theta)} = \upsilon(0^+,\theta) + \frac{1}{Pe}\frac{\partial \upsilon}{\partial \lambda}\bigg|_{(0^+,\theta)}\\
&\qquad\qquad \upsilon(0^-,\theta) = \upsilon(0^+,\theta)\\
&\text{Boundary Condition 2 :}\\
&\text{At}\quad \lambda = 1;\quad \upsilon(1^-,\theta) + \frac{1}{Pe}\frac{\partial \upsilon}{\partial \lambda}\bigg|_{(1^-,\theta)} = \upsilon(1^+,\theta) + \frac{1}{Pe}\frac{\partial \upsilon}{\partial \lambda}\bigg|_{(1^+,\theta)}\\
&\qquad\qquad \upsilon(1^-,\theta) = \upsilon(1^+,\theta)\\
&\text{where,}\quad \upsilon = x, h, \zeta
\end{aligned}$$

For a complete analysis of the aforementioned model such as the effect of the parameters $Pe$, $R$, $q$, and $\theta_\tau$ on the degree of hydrogenation (which is same 100 times conversion, $x$; refer Madhuranthakam et al.[5]).

*Manuscript received Nov. 27, 2008, and revision received Jan. 28, 2009.*